Available online at www.elixirpublishers.com (Elixir International Journal)

Mechanical Engineering

Elixir Mech. Engg. 191 (2025) 55109-55115

ISSN: 2229-712X

Influence of Anisotropy on the Modeling of Elastoplastic Phenomena in High Copper C18400 Alloys.

[1]Octavio R. Salazar San Andrés (External Researcher), [2]José María Rodríguez Lélis and [3]Oscar Domínguez Pérez
[1,2,3] Mechanical Department of National Center for Research and Technological Development from National Technologic of Mexico.

ARTICLE INFO

Article history:
Received: 11 June 2025;
Received in revised form:
3 July 2025;
Accepted: 28 July 2025;

Keywords
Anisotropy,
Elastoplasticity,
Mathematical Modeling

ABSTRACT

The present work carries out a study of resistance to deformation in materials from the point of view of anisotropy, for which a stress-strain analysis in tension and compression is presented, with the purpose of determining the corresponding elastic and plastic zones. The pure copper material called High Copper C1840 is used. Likewise, the relation of the anisotropic mathematical modeling of the deformation phenomena found is presented, obtaining the constants of Hooke's law, the characterization and analysis of the stress-strain curves, elasticity limit. A Mathematical Modeling is also proposed and the values of the mathematical model for the compression and tension process are contrasted with the reality of the experimentation obtained in the laboratory.

1. Introduction

The problem of fracture of materials in developed countries leads to annual losses close to 4% of the gross domestic product, as shown by statistics in the United States and the European community. Statistics on economic losses due to material fractures are difficult to compile in detail, but it is known that fractures, whether of materials or bones, have a significant cost. Corrosion, for example, is estimated to cost globally around $2.5 trillion, 3.4% of global GDP. [44].

The pioneers in the field of the strength of isotropic materials were Leonardo Da Vinci, Galileo Galilei and Robert Hooke, who proposed the hypothesis related to ultimate stress. He would later demonstrate, generalizing Galileo's concepts, that before breaking, a material goes through a series of states known as elasticity and plasticity. Cauchy and Navier formed the final theoretical formulation by proposing the constitutive equation, which was incorporated into Newton's second law previously developed by Euler, including two Lamé constants, related to Young's modulus and Poisson's modulus [34]. The study of anisotropy in materials dates back to the late nineteenth and early twentieth centuries with the study of the elastoplastic phenomenon [17].

Under this circumstance, and understanding that we have become more accurate in our operations by the computer finite element methodology based on Hooke's laws, but not more assertive to the knowledge of the elastoplastic phenomenon, the present work, proposes mathematical equations that model the deformation phenomenon in the elastoplastic transition of the solid.

1.1 Background

There was a break in the study of the anisotropy of materials from the mid 50's to the end of the 70's of the 20th centuries, which was subsequently resumed in the 90's. Thus, it could be stated that the strongest contribution is based on the work carried out by R. Hill (1948) [34], with his study of anisotropic plasticity [33]. However, Edelman R., Drucker D.C. (1951) present a detailed investigation of creep or loading criteria for strain hardening anisotropy materials[16]. The work of Atkinson, C., Clements D. L., (1977), relates to the analysis of constitutive equations in crack problems in anisotropic thermoelasticity [11]. Likewise, Harvery, S. J. (1985) uses an anisotropic plasticity approach to determine the plastic strains developed in two mechanical ratchet processes with tubes [31]. On the other hand, Kumar A., Samanta S.K., Mallick K. (1991) studied the change of orthotropy axes with consequent deformation to understand and interpret the subsequent creep behavior of metals. Based on Hill's hypothesis [40]. Likewise, Sadegh A.M., Cowin S.C. (1991) show, the six proportional invariants of an orthotropic elastic material using the elastic constants of spruce as a numerical example [51]. Ching S. Chang (1995), proposed an analysis of the Green's function for an elastic medium with general anisotropy [14]. For his part, G.A. Kardomateas (1995) proposed that, the equilibrium bifurcation of an orthotropic thick cylindrical sheet subjected to axial compression can be studied by an appropriate formulation based on the three-dimensional theory of anisotropic elasticity [24]. On the other hand, G. de Botton (1996) studied large magnitude plane-strain deformation involving a compressible orthotropic solid subjected to a uniaxial compressive load along one of the principal directions [14]. For his part, H. Murakami. (1996), investigated the effect of anisotropy and constitutive coupling of stretch, bending and transverse shear deformation on the deflection of a beam [30]. Related to the effective stress and in the description of anisotropic damage deformation within

the framework of continuum mechanics, G.Z. Voyiadjis (1997) defines a fourth order effective damage tensor [26]. On the other hand, Siguang Xu (1998) investigated the sheet forming limits using an anisotropic creep criterion, proposed by Hill (1993) [52]. Likewise, F. J. Montáns (2000)

formulated an anisotropic surface plasticity model with a deviatoric limit that preserves Masing's rule and an algorithm that considers the absence (or existence) of elastic range [20].On the other hand, Q. H. K. Truong and H. Lippmann (2001) analyzed isotropic and anisotropic hardening combined with plastic spin to describe the microstructural behavior of a polycrystalline metal in terms of continuum mechanics [49]. Likewise Bolke, A.Bertram, and E.Krempl (2003), developed a phenomenological model that accounts for the evolution of the elastic and plastic properties of fcc polycrystals. The anisotropic portion of the effective elastic tensor was modeled by a growth law, considering the dependence of the flow rule on the anisotropic part of the elastic tensor [55]. W. Tong, H. Tao, and X. Jiang (2004) present a simplified version of an anisotropic plasticity theory developed to describe the anisotropic flow behavior of orthotropic polycrystalline metallic films under uniaxial tension [58]. Similarly, C. Sansour, Kasaj and Soric (2007) developed a model and numerical algorithms that simulate the behavior of a material and the processes of forming and plastic deformation in general. [13]. Again, F. J. Montáns and M. A. Caminero (2007) briefly address the consistency of formulations for nested surface plasticity and their kinematic hardening translation rules, influenced by material anisotropy [19].

The work of M. A. Caminero Torija, (2010) The aim was to develop several tasks to improve the predictions of anisotropic kinematic hardening and the description of the initial elastoplastic anisotropy for anisotropic plasticity at large deformations [43]. On the other hand, Neupane, S., Adeeb, S., Cheng, R., Ferguson, J. and Martens, M. (2012) in their work related to pipe design, emphasize that high strength steel (HSS) pipes present plastic anisotropy, which cannot be incorporated in the traditional isotropic hardening plasticity model [47]. Likewise, Gao, E., Jia, X., Shui, L. and Liu, Z. (2021), made an interesting contribution based on the anisotropic approach of the material [27]. Finally, Tiantian Li, Yaning Li (2022) explore the anisotropic elastic mechanical properties of a family of single-material chiral mechanical metamaterials. An integrated monoclinic-micropolar constitutive model is developed to quantify the anisotropic mechanical properties of chiral designs with different geometries [42].

Previous works are very useful to understand the phenomenon of anisotropic deformation, however, not so many studies were found to demonstrate it in pure materials such as copper and particularly the material chosen for this research, copper C18400.

2. Mathematical Formulation

Starting from the considerations of the change of the quantity of movement according to Newton. The equilibrium equation is obtained, which relates surface and body forces, without considering temperature [17]:

$$\int_s \sigma^{ij} ds_i + \int_v \rho b^j dv = \frac{d}{dt}\int_v \rho u^j dv \qquad (1)$$

The surface forces are determined from the constitutive equation σ^{ij} **.** On the other hand, stress is not an isolated property, but is intrinsically related to the deformation of the material structure, and it has been shown that it can be represented as a second-order tensor from Hooke's law [20]. $\sigma^{ij} = C^{ijkl} \in^{kl}$ where C^{ijkl} it is a transformation tensor that relates stress and unit strain. For an isotropic medium it is concluded that

$$\sigma^{ij} = \lambda \delta^i_j \in_{kk} + 2\mu \in^{ij} \qquad (2)$$

where λ y μ are Lamé's constants [28]. The procedure for obtaining the Lamé constants is based on the fact that the material is anisotropic. By means of symmetry and orthotropy considerations, the transformation tensor C^{ijkl} which simplifies from eighty-one components to only two constants λ and μ [15].

3. Experimentation.

3.1 Selection of test material

The selected experimental material is high copper alloy type C18400. This is a commercial alloy, in demand in the industry.

3.2 Mechanical tests

In order to carry out a study of resistance to deformation in materials from the point of view of anisotropy, it is necessary to make a stress-strain analysis in tension, compression and torsion. The machinery used in the experimentation are: Universal machine MTS 810.; Instron 8500R.; Mitutoyo HR-350 hardness tester. The experimental procedure were standardized by ASTM standards [6], [3], [7], [8], [5], [9], [2], [1], [4], [29].

3.3 Characteristics of the mechanical tests.

Boundary conditions of Mechanical tests. (See Table 1 “Mechanical test conditions”)

4. Mathematical Analysis of Results

4.1 Obtaining the constants of Hooke's law

The elastic properties do not remain invariant to the orientation of the coordinate axes, therefore, it is necessary to find the values of the constants of the generalized Hooke's law, at least up to the orthotropic matrix.It is necessary to start from the values of Lamé's constants as a function of the engineering constants of the analyzed material.

Table 2. Orthotropy constants of Hooke's law

No	Constant (Hooke)	Constant, according to research	Value **in Pa.**
1	C_{11}	A	6.419 x 10^{10}
2	C_{22}	B	6.419 x 10^{10}
3	C_{33}	C	6.419 x 10^{10}
4	C_{44}	D	1.706 x 10^{10}
5	C_{55}	E	1.706 x 10^{10}
6	C_{66}	F	1.706 x 10^{10}
7	C_{12}	G	3.007 x 10^{10}
8	C_{21}	H	3.007 x 10^{10}
9	C_{13}	I	3.007 x 10^{10}
10	C_{31}	J	3.007 x 10^{10}
11	C_{23}	K	3.007 x 10^{10}
12	C_{32}	L	3.007 x 10^{10}

The engineering constants obtained from the experimentation are: Poisson's Coefficient: = 0.319; Young's modulus: E = 4.501x 1010 Pa.; Shear modulus: G = 1.706 x

1010 Pa. Substituting the values of Young's modulus and Poisson's modulus gives the Lamé constants: λ =3.007x10^{10} Pa & μ =1.706x10^{10} Pa. The corresponding the Lamé constants for these values are shown in Table 2 of orthotropy constants of Hooke's law.

With these values, the possibilities for predicting the behavior of copper increase considerably, since from the Lamé constants initially evaluated, it is translated into twelve constants. However, the anisotropic behavior cannot be predicted up to this point, since the transformation tensor is orthotropic. Nevertheless, it is a good approximation.

4.2 Characterization of stress-strain curves.

It was decided to characterize the curves of the elastic zone and the plastic zone separately in both tests and the approximations are the following:

For the elastic zone in compression, Figure 1.

$$\sigma = 948127\varepsilon - 1097.3 \quad (3)$$

And for plastic zone in compression, Figure 2.

$$\sigma = 79109\varepsilon^2 + 42714\varepsilon + 19878 \quad (4)$$

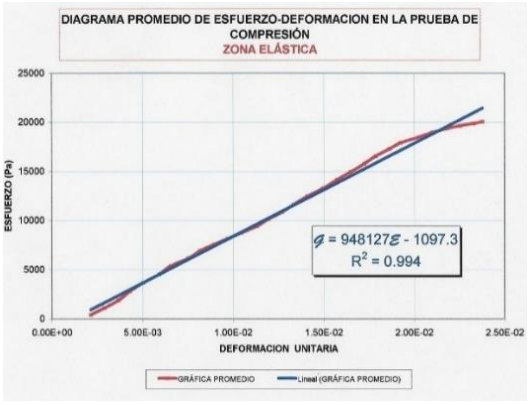

Figure 1. linear approximation in the elastic zone compression test.

Figure 2. Quadratic approximation for plastic zone compression test.

For the elastic zone in tension, figure 3. we have

$$\sigma = 5x10^{10}\varepsilon + 2x10^{7} \quad (5)$$

For the plastic zone in tension, figure 4. we have

$$\sigma = 9x10^{8}\varepsilon + 3x10^{8} \quad (6)$$

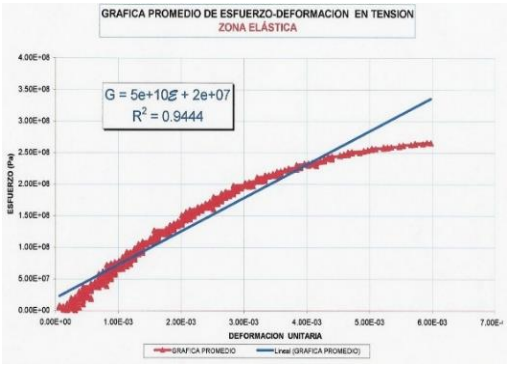

Figure 3. Elastic zone tension test. Linear approximation.

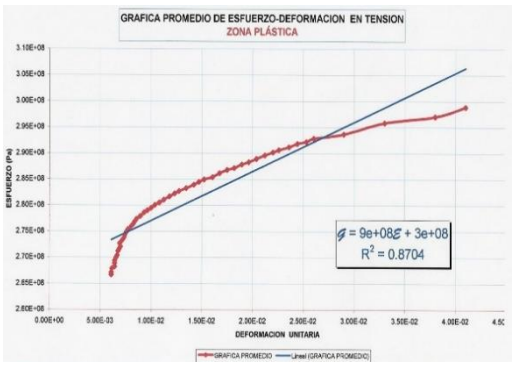

Figure 4. Plastic zone tension test. Linear approximation.

4.3 yield stress.

The yield stress for the tension and compression cases was obtained from the union of the two characteristic functions found corresponding to elasticity and plasticity. The criterion for joining both functions (elasticity and plasticity) in both deformation processes (tension and compression) was derived from the functions and their corresponding approximation equations, with a correlation coefficient closer to unity. The elastic limit corresponding to compression, by experimentation is the one with a unit strain ε equal to 2.2379x10-2 and a corresponding stress $\sigma\varepsilon$ equal to 20,072.57 Pa. The theoretical limit of elasticity in compression is

$$\varepsilon = 2.0961x10^{-2} \quad \sigma = 18776.7Pa \quad (7)$$

The explained error of both limits for compression is 11.9 % for ε and 6.45 % for, σ, Figure 5. The tensile yield strength of the copper studied in the experiment is defined by a value of 5.91 x 10-3 as unit strain and a stress of $\sigma\varepsilon$ 2.66 x 108 Pa. The values where the two functions meet at tension are:

$$\varepsilon = 5.71x10^{-3} \qquad \sigma = 3.05x10^{8}\,Pa \quad (8)$$

The explained error for this case was 3.38 % for ε and 12.9 % for σ, Figure 6.

Figure 5. The figure shows the elastic, theoretical and real limits found for pure copper in the compression test.

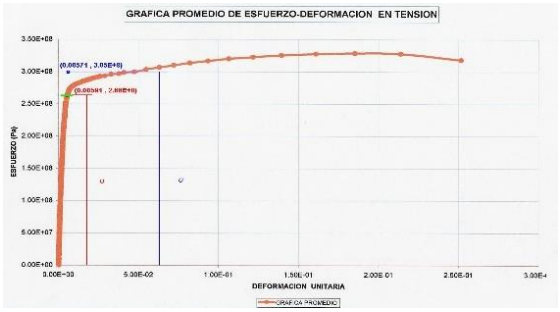

Figure. 6. The figure shows the elastic, theoretical and real limits found for pure copper in the tensile test.

5. Mathematical Modeling

This model is developed from the expression of change of quantity of motion expressed by Newton, in which the stress tensor is found . This tensor is related to the unit strain produced by the stress. The relationship found is the model that explains the behavior of the displacement as a function of the stress-preferential axis, which relates the unit strain of the deformation process in the elastic and plastic zones of the tension and compression phenomena by means of a single expression.

Based on the theory for continuous media [17], the following relation is the force balance equation in relation to the studied phenomenon.

$$\boldsymbol{\sigma_{ij,i} = \rho\left(\frac{\partial^2 u_j}{\partial t^2} + \frac{\partial u_i}{\partial t}\frac{\partial}{\partial X_i}\left(\frac{\partial u_j}{\partial t}\right)\right)\sigma_{ij.i} = \rho\left(\frac{\partial^2 u_j}{\partial t^2} + \frac{\partial u_i}{\partial t}\frac{\partial^2 u_j}{\partial X_i \partial t}\right)} \tag{9}$$

On the other hand, the approximation equations found in point 4 have a similar form to:

$$\sigma = a\varepsilon^2 + b\varepsilon + c \tag{10}$$

It is established as an important hypothesis that the deformation is corresponding to the elongation of the specimens in the experimental process:

$$\varepsilon = \frac{\partial u}{\partial z} \approx \frac{\Delta L}{L} \tag{11}$$

Since, the displacement is intrinsically related to the unit strain of the material in each of the tests performed. By taking the partial of equation (9) as a function of the Z-axis, we obtain:

$$\frac{\partial \sigma}{\partial z} = \rho\left(\frac{\partial^2 u}{\partial t^2} + \frac{\partial u}{\partial t}\frac{\partial^2 u}{\partial z \partial t}\right) \tag{12}$$

As "u" is assumed continuous, it is possible to use Shwarz's equality:

$$\boldsymbol{\frac{\partial^2 u}{\partial z \partial t} = \frac{\partial^2 u}{\partial t \partial z} \quad y \quad \frac{\partial \sigma}{\partial z} = \rho\left(\frac{\partial^2 u}{\partial t^2} + \frac{\partial u}{\partial t}\frac{\partial^2 u}{\partial t \partial z}\right)} \tag{13}$$

Similarly, and from (10):

$$\boldsymbol{\frac{\partial \sigma}{\partial z} = 2a\varepsilon\frac{\partial \varepsilon}{\partial z} + b\frac{\partial \varepsilon}{\partial z}; \quad s\acute{i} \quad \varepsilon = \frac{\partial u}{\partial z};} \tag{14}$$

$$\frac{\partial \sigma}{\partial z} = 2a\frac{\partial u}{\partial z}\frac{\partial^2 u}{\partial z^2} + b\frac{\partial^2 u}{\partial z^2} \tag{15}$$

Equating (14) and (15), neglecting the higher order terms, the final equation (which is a wave equation) remains:

$$\left(\frac{b}{\rho}\right)\frac{\partial^2 u}{\partial z^2} = \left(\frac{\partial^2 u}{\partial t^2}\right) \tag{16}$$

The boundary conditions are as follows:

$$u(0,t) = 0; \frac{\partial u}{\partial z}(0,t) = 0; \frac{\partial u}{\partial t}(0,t) = 0$$
$$\frac{\partial u}{\partial t}(L,t) = f; \frac{\partial u}{\partial z}(L,t) = h \tag{17}$$

being the initial conditions:

$$u(z,0) = 0; \frac{\partial u}{\partial t}(z,0) = 0 \tag{18}$$

Based on the boundary conditions, the initial conditions, the corresponding variable changes and the five-step method; integrating the phenomenon in the interval from "0 to L" equation (16) is solved as follows:

$$\boldsymbol{u = \sum_{n=0}^{\infty}\left\{2hL\left[\frac{1-\left(\frac{2n+1}{2}\right)\pi}{\left(\frac{2n+1}{2}\right)\pi}\right]sen\left(\frac{2n+1}{2}\right)\frac{\pi z}{L}cos\left(\frac{2n+1}{2}\right)\sqrt{\frac{b}{\rho}}\frac{\pi t}{L}\right\} + hz} \tag{19}$$

therefore, from equations 11 and 19, we have:

$$\varepsilon = \frac{\partial u}{\partial z} = \sum_{n=0}^{\infty}\left\{2hL\left[\frac{1-\left(\frac{2n+1}{2}\right)\pi}{\left(\frac{2n+1}{2}\right)\pi}\right]\left(\frac{2n+1}{2}\right)\frac{\pi}{L}\cos\left(\frac{2n+1}{2}\right)\frac{\pi z}{L}\cos\left(\frac{2n+1}{2}\right)\sqrt{\frac{b}{\rho}}\frac{\pi t}{L}\right\} + h \tag{20}$$

This last relation is the model that explains the behavior of the displacement as a function of the preferential z-axis. In addition, it relates the unit strain of the deformation process in the elastic and plastic zones of the two phenomena of tension and compression respectively.

6. Analysis and calculations of the mathematical model.

The mathematical model suggested in the research was tested with the following boundary conditions: a) Length of the specimen: 0.175m; b) Density of pure copper: 8931.66 kgm/m3; c) Test time: up to 600-900 seconds. Also, to

determine the value of the constant of the equation to be used in each analysis, it was necessary to consider that the deformations are small and therefore, the quadratic or cubic terms are disregarded and only the values of the constant that is related to the linear terms of each approximation equation are taken (3,4,5,6).

6.1 Values of the mathematical model for the compression process.

In this analysis, the test was taken up to a time of 1080 seconds. The time variation was taken as a function of the experimental test, since the amount of data obtained in the actual deformation of the specimen is directly proportional to the time in which the test is carried out. In the case of the compression phenomenon, the elastic part has a considerable deformation time, so small time intervals from 0 to 60 seconds were left. After this time, the intervals were taken in periods of 60 seconds. The frequency of model testing was equal to the number of times required, because it depends on the intervals where the model acquires data or intervals characteristic of the elastoplastic phenomenon function. In this case the frequency is equal to 24 runs.

The iteration is the value of n stated in equation (20), this being the value of the number of summations performed and denotes the increase of the function in the deformation process. This value gives valuable information since the function is a wave equation where many values obtained are cyclic. The maximum value of n in this calculation was 109 and the minimum was 0.

The experimentation shows how the material deforms before the imminent effort that supports the material product of a surface force. With the model suggested in the research, it is intended to find the way in which the material would behave without the need to physically perform the corresponding test. This is the reason why it is necessary to compare the data obtained in the model and those obtained through experimentation. For this purpose, the model data were plotted against the experimental data and the standard deviation of the values obtained was calculated.

It is notoriously observed that the data obtained in the suggested model are close to the real ones obtained by experimentation, Figure 7, where the suggested equation (20) perfectly models the elastoplastic phenomenon in the compression deformation process**.**

Figure 7. Comparative graph of the real values obtained in the experimentation, against the values calculated by the mathematical model. Compression test.

6.2 Values of the mathematical model for the tension process.

In this analysis, 22 frequencies with strain values of the order between 5.65x10-4 and 2.44x10-1 were performed, these values correspond to the interval found in the average stress-strain curve in compression. The stress was calculated by the approximation curves obtained previously.The comparison of the data obtained in the model and by experimentation is shown in the graphs in Figures 8 and 9. Both curves represent the elastoplastic phenomenon in tension, the difference lies in the fact that one is the average curve of 23 specimens broken in the experiment (Fig. 8) and the other is the curve of specimen 17, which recorded the maximum stress performed (Fig. 9).

The mathematical model suggested in the investigation accurately calculates the elastic behavior, crosses the yield point and models with good approximation the change of direction of the curve in the elastoplastic transition zone. However, when the plasticity of the material is more evident, the graph of equation (20) projects linearly and increases progressively away from the real stress-strain curve obtained experimentally (Fig. 8 and Fig. 9).

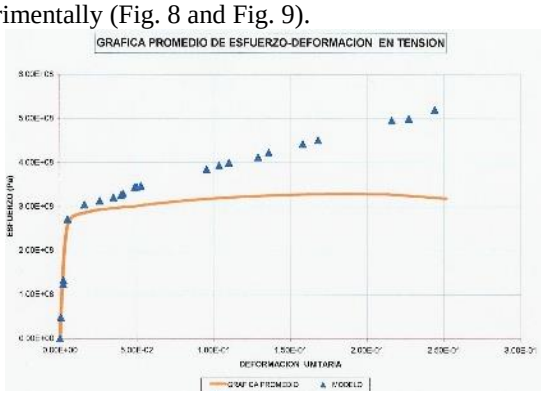

Figure8. Comparative graph of the real values obtained in the experimentation, against the values calculated by the mathematical model in the tensile deformation process. The graph shows the average experimental stress-strain curve.

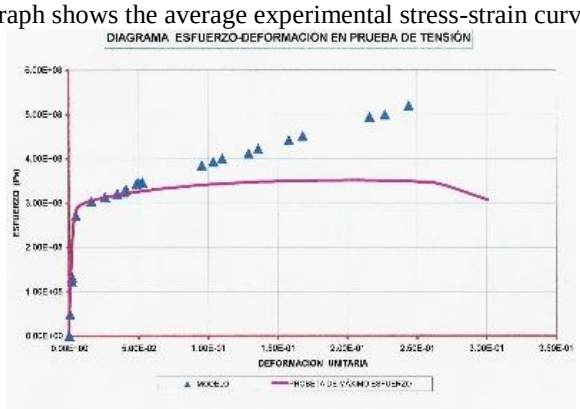

Figure 9. Comparative graph of the real values obtained in the experimentation, against the values calculated by the mathematical model in the tensile deformation process. The graph shows the experimental stress-strain curve for specimen 17, which records the maximum stress

This sudden variation of the model, with respect to the real curve, generates doubts about its application in tensile deformation processes. However, even with these differences in the model, it behaves in a stable manner in the elastic zone, and also describes the characteristic curve and therefore the transition process from the elastic to the plastic zone.

Conclusions.

Modeling the elastoplastic phenomenon from the point of view of anisotropy is possible. Since equation (20) obtained is the model that explains the behavior of the displacement as a function of the preferential z-axis. In addition, it relates the unit strain of the deformation process in the elastic and plastic zones of the two phenomena of tension and compression respectively. This expression, when modeled and compared with experimental data, shows excellent performance in compression and medium performance in tension. The fundamental reason for this is that in the compression deformation process the granular structure is compacted. That is, compressed in such a way that the propagation of the perturbation resulting from the deformation is not altered and the propagation velocity remains constant. On the other hand, in the tension process, the granular structure is totally deformed, thus generating that the propagation of the perturbation, product of the deformation, is altered and as a consequence the propagation velocity of the same is altered.

Future work will be aimed at testing the model with other materials, after improving it in the tension process, in order to better model the elastoplastic phenomenon in the deformation phenomenon of the material.

Table 1. Mechanical test conditions.

Type of Test	Maximum Force. N	Velocity mm/seg or rpm	No. of specimens	Humidity %	Average Temperature ^{o}C
Tension	52590.25	0.5	30	25	19
Compression	1008.88	0.5	20	28	21
Torsion	20820.14	2-8 rpm	20	39	24

Bibliography

[1] [ASTM E565.01] ATM Designation: B 565., Revised 2017. “Standar Method for Shear Testing of Aluminum and Aluminum Alloy Rivets and Cold-Heading Wire and Rods”.

[2] [ASTM E9.00] ASTM. Designation: E9., “Standar Methods of Compression Testing of Metallic Materials at Room Temperature”. Revised 2018.

[3] [ASTM. E132.00] ASTM. Designation: E132. Revised 2022, “Standar Method of Test for Poisson’s Ratio at Room Temperature”.

[4] [ASTM. E228.00] ASTM Designation: E 228. Revised 2021, “Standar Method of Test for Linear Thermal Expansion of Solid Materials With a Vitreous Silica Dilatometer”.

[5] [ASTM. E6.00] ASTM. Designation: E6. Revised 2023A, “Standar Definitions of Terms Relating to Methods of Mechanical Testing.

[6][ASTME111.00] ASTM. Designation: E 111-17., “Standar Method of Test for Young’s Modulus at Room Temperature”. Revised 2017.

[7] [ASTME143.01] ASTM. Designation: E 143-02., “Standar Method of Test for Shear Modulus at Room Temperature”. Revised 2021.

[8] [ASTME4.00] ASTM. Designation: E4., “Standar Methods of Verification of Testing Machines”. Revised 2024.

[9] [ASTME8.00] ASTM. Designation: E8., “Standar Methods of Tension Testing of Metallic Materials”. Revised 2024.

[10] [IEEE/ASTM SI 10] Estándar nacional estadounidense para la práctica métrica. 2017. Vol. 14.04, Subcomité E43.10. ICS:01.060;01.120.

[11] Atkinson, C.,Clements D. L., 1977, "On Some Crack Problems in Anisotropic Thermoelasticity" J. Solids structures. Vol 13.

[12] C. W. Fan. March 1996 “Punch Problems for an Anisotropic Elastic Half-Plane”.ASME, vol 63,

[13] C.Sansour, I.Kasaj, and J.Soric, “On anisotropic flow rules in multiplicative elastoplasticity at finite strains,” Computers Methods in Applied Mechanics and Engineering, vol. 196, pp. 1264—1309, 2007.

[14] Ching S. Chang. 1995, “Green’s Function for Elastic Medium with General Anisotropy”. ASME, vol. 62, September.

[15] Demenedhi A., Magana R., Sángines H. Apuntes de Mecánica del Medio Continuo. UNAM 2000. Primera edición.

[16] Edelman R., Drucker D.C. 1951, "Some Extensions of Elementary plasticity". J of Franklin Institute. Vol 251, No. 6.

[17] Enzo Levi. 1994 “Mecánica del Medio Continuo”., Ed. Limusa, Mexico.

[18] F. A. Sturla , J. R. Barber. June 1988, "Termal Stresses Due to a Plane Crack in General Anisotropic Material". ASME J. of Engenering Materials and Technology. Vol. 55.

[19] F.J. Montáns and M.A.Caminero, “On the consistency of nested surfaces models and their kinematic hardening rules,” International Journal of Solids and Structures, vol. 44, pp. 5027—5042, 2007.

[20] F.J. Montáns, “Bounding surface plasticity model with extended masing behaviour,” Computer Methods in Applied Mechanics and Engineering, vol. 182, pp. 135—162, 2000.

[21] G. deBotton. June 1996, “Bifurcation of Orthotropic Solid”. ASME, vol 63,

[22] G. Medri , Junary 1982.." A Nonlinear Elastic Model For Isotropic Materials With Different Behavior in Tension and Compression". ASME. Journal of Engineering Materials and Technology vol. 104.

[23] G.A. Holzapfel, Non-linear Solid Mechanics. England: Wiley, 2000.

[24] G.A. Kardomateas. March 1995. “Bifurcation of Equilibrium in Thick Orthotropic Cylindrical Shells Under Axial Compression”. ASME, vol. 62,.

[25] G.R. Liu. September 1995 “Strip Element Method to Anayze Wave Scattering by Cracks in Anisotropic Laminated Plates”. ASME, vol. 62.

[26] G.Z. Voyiadjis March 1997. “Anisotropic Damage Effect Tensors for the Symmetrization of the effective Stress Tensor”., ASME vol 64.

[27] Gao, E., Jia, X., Shui, L. and Liu, Z. (October 27, 2020). "Tuning nonlinear mechanical anisotropy of layered crystals by interlaminar torsion". ASME. J. Appl. Mec . Jan. 2021; 88(1): 011007.https://doi.org/10.1115/1.4048647
[28] George E. Mase. "Mecanica del Medio Continuo1978.".,Ed. McGraw-Hill., México.
[29] Gutiérrez-Pulido, H. & De la Vara-Salazar, R. (2012). Análisis y diseño de experimentos. México: McGraw Hill.
[30] H. Murakami. 1996, "Anisotropic Beam Theories with Shear Deformation". ASME vol 63, September.
[31] Harvery, S.J. 1985. "The Use of Anisotropic Yield Surface in Cyclic Plasticity" ASTM STP 853. pp 49-53.
[32] Hill R. 1979. "Theoretical Plasticity of Texture Aggregates" Math. Pro. Camb. Phil. Soc. , Vol. 85 .
[33] Hill R., 1950., " The Mathematical Theory of Plasticity ", Clarendon . Oxford.
[34] Hill, R. 1948. "A Theory of the yield and Plastic Flow of Anisotropic Metals" Proc. Royal Soc.,London A193.
[35] Hwei P. Hsu. 1987 "Analisis Vectorial". Ed. Addison-Wesley Iberoamericana. Wilmington, Delaware, EUA,.
[36] Ikegami K. 1979. "Experimental Plasticity on the Anisotropy of Metals , Simposium of Mechanical Behavior of A nisotropic Solids." France, ed Boehler , J.P., pp 201-244.
[37] James W. Dally, William F. Riley. 2015. "Experimental Stress Analysis". Ed. McGraw-Hill. New York.,
[38] Joseph E. Shigley. 1997, "Standard Handbook of Machine Desing". Ed. McGraw-Hill, Inc. New York.,.
[39] Kenneth G. Budinski, 1996. "Engineering Materials Properties and Selection". Prentice Hall. Columbus, Ohio.
[40] Kumar A., Samanta S.K., Mallick K. Aprl 1991" Study of The Effect of Deformation on the Axes of Anisotropy". ASME. J. Engineering Materials and Technology". Vol 113.
[41] Lawrence E. Doyle., 1985 " rocesos y Materiales de Manufactura para Ingenieros ". Ed. Prentice-Hall Hispanoamericana, S. A., México.
[42] Li, T. and Li, Y. (September 9, 2022). "Anisotropy prediction of chiral mechanical metamaterials by micropolar modeling". ASME. J. Appl. Mec. Oct. 2022; 89(10): 101006. https://doi.org/10.1115/1.4055349.
[43] M. Á. Caminero Torija. 2010 Elastoplasticidad Anisótropa de Metales En Grandes Deformaciones. I.S.B.N. Ediciones de la UCLM 978-84-8427-772-9. Cuenca, 2010.
[44]Maysa Barbosa. 12 de marzo de 2025. https://hmrubber.com.uy/la-corrosion-en-cifras-impacto-global-y-soluciones-efectivas/ /#:~:text.
[45] Metals Handbook 1998. American S0ciety for Metals, Vol 5, Vol 7.
[47] Movnin M. S.,Rubashkin A. G. 2000.; Fundamentos de mecánica Técnica. Ed. Mir Moscú.
[48] Neupane, S., Adeeb, S., Cheng, R., Ferguson, J. and Martens, M. (June 21, 2012). "Modeling the deformation response of high strength steel pipes - Part I: Material characterization for modeling plastic anisotropy". ASME. J. Appl. Mec. Sep. 2012; 79(5): 051002. https://doi.org/10.1115/1.4006380.
[49] P. Gutiérrez, H. & De la Vara-Salazar, R. (2012). Análisis y diseño de experimentos. México: McGraw Hill.
[50] Q.H.K.Truong and H.Lippmann, "Plastic spin and evolution of an anisotropic yield condition," International Journal of Mechanical Sciences, vol. 43, pp. 1969—1983, 2001.
[51] S.A. Matemilola. September 1995. "Diffusion Rate for Stress in Orthotropic Materials". ASME, vol 62,.
[52] Sadegh A.M., Cowin S.C., March 1991" The Proportional Anisotropic Elastic Invariants". ASME. J. of Engineering Materials and Technology" Vol 58.
[53] Siguang Xu. 1998. "Analysis of Forming Limits Using the Hill 1993 Yield Criterion". ASME vol. 120, July 1998.
[54] Sydney H. Avner. 1988., "Introducción a la Metalurgia Física ". Ed. McGraw-Hill., México,
[55] T. Takeda. Junary 1993 " Yield and Flow Behavior of Initially Anisotropic Aluminum Tube Under Multiaxial Stresses". ASME, Journal of Engeneering Materials and Technology. vol. 115.
[56] T.Bolke, A.Bertram, and E.Krempl, "Modelling of deformation induced anisotropy en free-end torsion," International Journal of Plasticity, vol. 19, 2003.
[57] Takeda, T. 1991, "The aplications of Anisotropic Yield Function of The Six Degree to Orthotropic Materials". J strain Analysis, Vol 26 pp 345.
[58]Thompsom M., Willis J.R. 1991 " A Reformation of the Equations of Anisotropic Poroelasticity". ASME. J. of Engineering Materials and Technology. Vol 58, September.
[59] W.Tong, H.Tao, and X.Jiang, "Modeling the rotation of orthotropic axes of sheet metals subjected to off-axis uniaxial tension," Journal of Applied Mechanics ASME, vol. 71, pp. 521—531, 2004.